ELECTRON-CLOUD MEASUREMENTS AND SIMULATIONS FOR THE APS[*]

M. A. Furman and M. Pivi, LBNL, Berkeley, CA 94720, USA[†]

K. C. Harkay and R. A. Rosenberg, ANL, Argonne, IL 60439, USA[‡]

Abstract

We compare experimental results with simulations of the electron cloud effect induced by a positron beam at the APS synchrotron light source at ANL, where the electron cloud effect has been observed and measured with dedicated probes. We find good agreement between simulations and measurements for reasonable values of certain secondary electron yield (SEY) parameters, most of which were extracted from recent bench measurements at SLAC.

1 INTRODUCTION

The electron-cloud effect (ECE) has been observed or is expected at many storage rings. It is generally a limiting factor in the performance of the machine, via collective instabilities, particle losses, enhanced vacuum pressure, or emittance blow-up. Computer simulation codes have been developed over the past few years to investigate the ECE and try to predict its importance in future machines [1, 2]. In parallel, electron detectors have been designed and built at ANL [3] to study the electron cloud experimentally, and have been tested and installed at the APS [4] and the PSR at LANL [5].

In this article we present a direct, controlled comparison between measurements obtained at the APS and results from the LBNL simulation code [6, 7]. Specifically, we consider the intensity of the electrons hitting the walls of the vacuum chamber in a field-free region, when the APS was operated with a positron beam. Although the electron detectors can also measure the energy spectrum of the electrons, we focus here only on the intensity of the electron signal. We shall present a more complete set of results, including those for the case of an electron beam, in a future publication [8].

2 ELECTRON DETECTORS

A compact, planar retarding-field analyzer (RFA) was constructed [3] for the diagnostics of low-energy background electrons in high-energy particle accelerators. The RFA consists of two 70-lines/inch (90% transmission) copper grids and a collector. The first grid is grounded to present a uniform field to the incoming electrons. The second grid is biased at a retarding potential, E_v, such that only electrons with kinetic energies greater than E_v are

transmitted to the collector. The collector is coated with graphite to lower the SEY, and is biased at 45 V with a battery to increase the collection efficiency. The assembled detector is mounted behind a slotted vacuum penetration on a 2.75-in Conflat flange with two electrical feedthroughs. The collection area is $\sim 1\ \mathrm{cm}^2$. Figure 1 shows the location of the detectors as mounted on a standard APS aluminum vacuum chamber. A total of ten detectors were mounted along the length of a 5-m straight chamber in a field-free section.
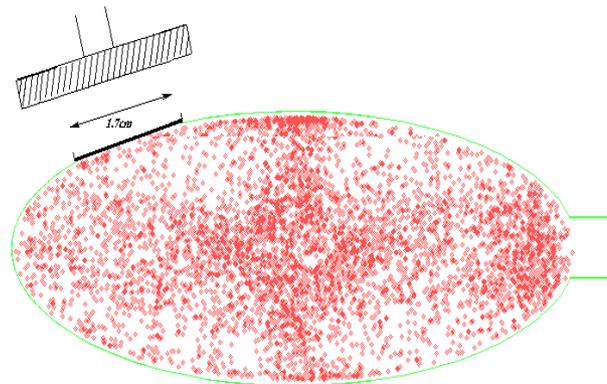

Figure 1: Schematic showing the location of a RFA on the APS vacuum chamber. The red dots in the chamber represent electron-cloud macroparticles in a snapshot of a digital movie of the simulation.

For the purposes of comparison with simulation, data from a detector near the middle of the 5-m chamber was chosen. The detector is 9.2-m downstream from the end of a bending magnet (11.9 m from the source point) and 0.76 m upstream from an end absorber (EA), whose purpose is to intercept photons. The detector is minimally affected by photoelectrons produced at the EA. However, proximity to the EA does influence the detector signal when there is amplification by secondaries, as under beam-induced multipacting conditions. At the time the data were acquired, 98 A-h of beam operation had accumulated since the detectors were first installed and 1 A-h since the chamber vented to air. The chamber undergoes a standard bake-out procedure after venting.

679

Table 1: Simulation parameters for the APS.

Parameter	Symbol	Value
Circumference	C	1104 m
Harmonic number	h	1296
RF frequency	f_{RF}	351.93 MHz
Beam energy	E	7 GeV
Bunch population	N_p	4.6×10^{10}
RMS bunch length	σ_z	5 mm
Trans. RMS bunch sizes	σ_x, σ_y	300,50 μm
Beam pipe semiaxes	a, b	4.25,2.1 cm
Antechamber slot height	h	1 cm
Eff. photoelectric yield	Y'	0.1
No. of photons	N_γ	7×10^{-2}
SEY params.	δ_{max}, E_{max}	3.3, 280 eV
Number of kicks	N_k	5

3 SIMULATION

3.1 Sources of Electrons

In the studies presented here we fixed the bunch current at 2 mA/bunch, corresponding to 4.6×10^{10} particles per bunch, and we also fixed the number of bunches in the beam at 10. We did vary the bunch spacing n_{sb} in the range $1 \leq n_{sb} \leq 128$ (measured in units of RF buckets) while we kept the bunch spacing fixed within the train.

In this article we consider only what we believe to be the main two sources of electrons, namely: (1) photoelectrons arising from the synchrotron radiation hitting the walls of the vacuum chamber, and (2) secondary emission from electrons hitting the walls. Although our code accommodates other sources of electrons, such as residual gas ionization, we have turned them off for the purposes of this article.

We represent the SEY $\delta(E_0)$ and the corresponding emitted-electron energy spectrum $d\delta/dE$ (E_0 =incident electron energy, E = emitted secondary energy) by a detailed model described elsewhere [6, 7]. Its parameters were obtained from detailed fits to the measured SEY and spectrum of Aluminum [9]; however, we note that these measurements were not done on samples from the APS vacuum chamber, hence there is a certain amount of uncertainty in the actual values used as input to our simulations. The main parameters are the energy E_{max} at which $\delta(E_0)$ is maximum, and the peak value itself, $\delta_{max} = \delta(E_{max})$ (see Table 1).

3.2 Simulation Model

For the positron bunch we assume a 3D Gaussian distribution with rms sizes σ_x, σ_y, σ_z. We simulate the passage of the beam in a field-free section with a vacuum chamber assumed to be perfectly conducting and of elliptical cross-section with an antechamber slot of full height h. Photoelectron generation by photons hitting the wall is repre-

sented by the product of two parameters, $Y' \times N_\gamma$, where Y' is the effective photoelectric yield per penetrated photon, and N_γ is the number of photons hitting the wall of the chamber whose energy is above 4 eV, per bunch passage and per positron in the beam (photons that go out to the antechamber are not counted). We assume that the generated photoelectron time distribution is proportional to the instantaneous bunch intensity.

The electrons are then simulated by macroparticles. We typically use 100 macroparticles per bunch passage to represent the photoelectrons in the section being simulated. The secondary electron mechanism adds to these a variable number of macroparticles, generated according to the SEY model mentioned above. The bunch is divided up into slices, so that the macroparticles experience N_k kicks during the bunch passage. We also divide the empty buckets into N_g intermediate steps. The space-charge forces are calculated and applied at each kick in the bunch, and at each step in an empty bucket. The image forces of both the beam and the electrons are taken into account, assuming a perfectly conducting wall. Typical parameter values are shown in Table 1.

Fig. 2 shows the measured and simulated RFA current, averaged over one revolution period.
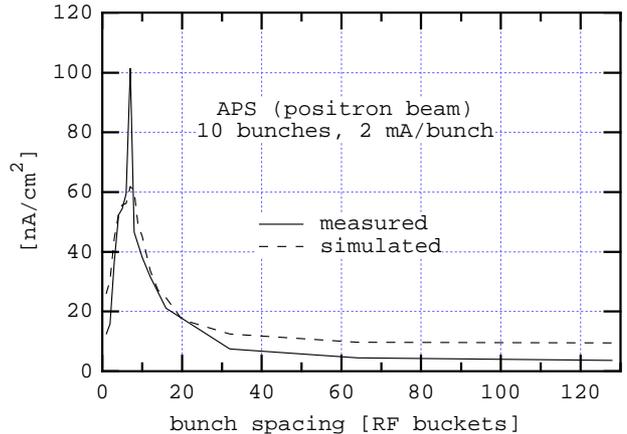

Figure 2: Measured and simulated electron-detector current. The measured data is the RFA current at the maximum signal (E_v near 45 V), *i.e.*, such that electrons of all energies are counted. The simulated data assumes unit detector efficiency and acceptance.

4 RESULTS AND DISCUSSION

The simulation results are in good qualitative agreement with experimental data. There are, however, two clear quantitative discrepancies: (1) the measured data shows a large spike at $n_{sb} = 7$ whose height is not well reproduced by the simulation, and (2) the measured current level at large bunch spacing, $n_{sb} > 32$, is $\sim 50\%$ of the simulated values.

The peak at $n_{sb} = 7$ is almost certainly due to beam-induced (resonant) multipacting. A simple formula [10] gives an estimate for the value of the bunch spacing for which the resonance condition is met. For an elliptical cross-section chamber of semi-axes (a, b), it is

$$s_B = \frac{d^2}{N_p r_e} \qquad (1)$$

where s_B is the bunch spacing (in units of length), $r_e \simeq 2.82 \times 10^{-15}$ m is the classical electron radius, and d is in the range $b \lesssim d \lesssim a$. This formula yields the range $4 \lesssim n_{sb} \lesssim 16$, consistent with the data in Fig. 2. This equation is derived under simplifying assumptions that do not exactly correspond to the actual simulation. The simulation, on the other hand, embodies the multipacting phenomenon in all its details, and we are satisfied that it yields a clear maximum at $n_{sb} = 7$. Unfortunately, however, we do not know any simple formula that yields the *height* of the current peak at resonance, hence we do not have an approximate expectation for the simulation result, hence the discrepancy at $n_{sb} = 7$ remains to be better understood. We note, however, the the measured height of the peak decreased significantly when the measurements were repeated at a later date, after a surface conditioning effect took place.

At large n_{sb} the SEY plays a very weak role because the bunch separation is large enough that the electron cloud substantially clears during the interbunch gap, hence the photoelectrons have a small probability to get amplified by the SEY phenomenon. Indeed, we have verified that the simulated current changes little for $n_{sb} > 32$ when we fully switch off the SEY. We have also verified that, for these large bunch spacings, the simulated electron current scales quite linearly with the photoelectric yield, as it should be expected. We believe that the discrepancy will be explained by details of the detector acceptance and efficiency. Although the RFA transmission has been measured at 80%, and its angular acceptance has been quantified for bench measurements [3], we have not yet included these details in the simulations, for which we assumed perfect RFA acceptance and efficiency. Indeed, the simulations show that, for small n_{sb}, the electrons, on average, collide with the wall preferentially at normal incidence, while at large bunch spacings they do so with a wide angular spectrum, roughly centered at $\cos\theta \simeq 0.6$ ($\theta =$collision angle, normal incidence is $\cos\theta = 1$). Furthermore, our simulation computes only an average (transversely and longitudinally) of the electron-wall current around the chamber, whereas the electron cloud can, in fact, have substantial variations as a function of location in the chamber. These details will be studied in the future [8]. It is clear, however, that, overall, the simulations offer a good explanation of the observations.

5   ACKNOWLEDGMENTS

6   REFERENCES

[1] For a summary, see Proc. ICFA Workshop on Two-Stream Instabilities, Santa Fe, NM, Feb. 16–18, 2000, http://www.aps.anl.gov/conferences/icfa/two-stream.html

[2] G. Rumolo, F. Ruggiero and F. Zimmermann, PRST-AB **4**, 012801 (2001) (erratum: **4**, 029901 (2001)). See also F. Zimmermann, these proceedings.

[3] R. A. Rosenberg and K. C. Harkay, NIMPR **A453** (2000), 507–513.

[4] K. Harkay and R. Rosenberg, Proc. PAC99, p. 1641.

[5] R. Macek, these proceedings.

[6] M. A. Furman and G. R. Lambertson, Proc. Intl. Workshop on Multibunch Instabilities in Future Electron and Positron Accelerators (MBI-97), KEK, Tsukuba, Japan, 15-18 July 1997 (KEK Proceedings 97-17, Dec. 1997, p. 170); http://www.lbl.gov/~miguel/MBI97-ECI-PEPII.pdf

[7] M. A. Furman, LBNL-41482/CBP Note 247/LHC Project Report 180, May 20, 1998, http://www.lbl.gov/~miguel/LHCpr180.pdf

[8] M. A. Furman, M. Pivi, K. C. Harkay and R. A. Rosenberg, to be published.

[9] R. Kirby, private communication.

[10] O. Gröbner, Proc. 10th Intl. Accel. Conf., Serpukhov, 1977, pp. 277–282.